Multi-Targeting Approach in Selection of Potential Molecule for COVID-19 Treatment

Varalakshmi Velagacherla
Manipal College of Pharmaceutical Sciences, Manipal Academy of Higher Education, Manipal, India
Akhil Suresh
Manipal College of Pharmaceutical Sciences, Manipal Academy of Higher Education, Manipal, India
https://orcid.org/0000-0001-8184-5125
Chetan H Mehta
Manipal College of Pharmaceutical Sciences, Manipal Academy of Higher Education, Manipal, India
https://orcid.org/0000-0002-1895-8562
Yogendra Nayak
Manipal College of Pharmaceutical Sciences, Manipal Academy of Higher Education, Manipal, India
https://orcid.org/0000-0002-0508-1394
Usha Y Nayak (usha.nayak@manipal.edu)
Manipal College of Pharmaceutical Sciences, Manipal Academy of Higher Education, Manipal, India
https://orcid.org/0000-0002-1995-3114

Research Article

Keywords: SARS-CoV-2, Molecular docking, Prime MM-GBSA, Induced fit docking, Molecular dynamics simulation

Posted Date: November 3rd, 2020

DOI: https://doi.org/10.21203/rs.3.rs-101359/v1

Abstract

Background: Coronavirus disease (COVID-19) caused by the severe acute respiratory syndrome coronavirus-2 (SARS-CoV-2) is now a pandemic which began in Wuhan province of China. Drug discovery teams around the globe are in a race to develop a medicine for its management. For a novel molecule to enter into the market it takes time and the ideal way is to exploit the already approved drugs and repurpose them to use therapeutically.

Methods: In this work, we have attempted to screen selected molecules that have shown an affinity towards multiple protein targets of COVID-19 using Schrödinger suit. Molecules were selected from approved antiviral, anti-inflammatory or immunomodulatory classes. The viral proteins selected were angiotensin-converting enzyme 2 (ACE2), main protease (M^{pro}) and spike protein. Computational tools such as molecular docking, prime MM-GBSA, induced-fit docking (IFD) and molecular dynamics (MD) simulations were used to identify the most suitable molecule that forms a stable interaction with the selected viral proteins.

Results: The ligand-binding stability for the viral proteins PDB-IDs 1ZV8 (spike protein), 5R82 (M^{pro}) and 6M1D (ACE2), was in the order of Nintedanib>Quercetin, Nintedanib>Darunavir, Nintedanib> Baricitinib respectively. The MM-GBSA, IFD, and MD simulation studies infer that the drug nintedanib has the highest binding stability among the shortlisted molecules towards the selected viral target proteins.

Conclusion: Nintedanib, which is primarily used for idiopathic pulmonary fibrosis, can be considered for repurposing and used in the management of COVID-19.

Introduction

Novel coronavirus disease (COVID-19) was first identified in Wuhan, a city in China. The first case was reported in December 2019, and the virus attacked an elderly woman who was 54 years old and was later diagnosed as severe acute respiratory distress syndrome having asthenia, fever and other respiratory difficulties such as low respiratory rate and less frequency of saturated oxygen in the body. The virus was first named as ‘novel coronavirus’ (nCoV), and later nomenclature was made as ‘severe acute respiratory syndrome corona virus-2’ (SARS-CoV-2). The World Health Organization declared this pandemic disease by SARS-CoV-2 as COVID-19 [1]. Severe acute respiratory syndrome (SARS), Middle Eastern respiratory syndrome (MERS) and COVID-19 are zoonotic and have shown bats as a common origin, all the three viral diseases share common symptoms, they are diagnosed by taking nasal, or throat swab then use real-time reverse transcriptase-polymerase chain reaction to determine the presence of viral genetic material [2]. Person to person transmission of SARS-CoV-2 occurs via nasal droplets, by direct contact with infected patient or materials and surfaces used and touched directly by the infected person. Major symptoms seen in COVID-19 patients are fever, cough, fatigue, headache, cardiac injury, hypoxemia, lymphopenia, dyspnoea, diarrhoea, rhinorrhea, pneumonia, respiratory distress syndrome, sore throat, sneezing and RNAaemia [3]. SARS-CoV-2 gains access to the body via the nose, mouth, or eyes, and from

there it moves into alveolar sacs and further to alveolar cells of lungs. After the virus enters the lungs, it uses its spike glycoprotein to enter into cells. Spike protein (S-protein) of coronavirus composes of transmembrane glycoprotein which is trimetric in nature and protrudes from the surface of the virus. The viral S-protein has a high affinity to ACE2 receptors mainly in type-II alveolar cells, the virus then gets internalized by membrane fusion or endocytosis [4]. The main protease (M^{pro}) is a viral protease which activates a series of events with RNA-dependent RNA polymerase (RdRp) which helps in replication of the viral genetic material and make multiple virus copies [5]. Hence, S-protein, ACE2, M^{pro} and RdRp are important druggable targets in drug discovery.

SARS-CoV-2 proteins are of two classes, structural and non-structural proteins (nsp). The non-structural proteins include M^{pro}, papain like protease (PLpro), nsp13 (also known as helicase), nsp12 (also known as RdRp), nsp14 (also known as N-terminal exoribonuclease and C-terminal guanine-N7 methyltransferase), nsp15 (also known as uridylate-specific endoribonuclease), nsp16 (also known as 2'-O-methyltransferase), and nsp10 while the structural proteins includes S-protein, envelop small membrane protein (E), membrane protein (M), and nucleocapsid protein (N) [6]. Clinical trials are ongoing to identify a suitable drug molecule which can combat the problems associated with COVID-19 [7]. Though the repurposing of drugs like remdesivir, favipiravir and dexamethasone have been approved for treatment of COVID-19, they have major limitations and there is no complete cure [8].

Computational modelling helps to identify a potentially useful molecule from a large library of molecules in less time by using various tools such as molecular docking, Prime molecular mechanics generalized Born surface area (Prime MM-GBSA), induced-fit docking (IFD) and followed by molecular dynamic (MD) simulation for the selected molecules. Elfiky et al. 2020, have selected some anti-hepatitis-C drugs and performed computational studies like molecular docking, and MD simulations in order to check the efficacy of these drugs on RdRp [9]. Results have shown that some of the drug moieties have better stability and binding affinity towards SARS-CoV-2 RdRp. Sahu et al. 2020, have worked by taking SARS-CoV-2 $3CL^{pro}$ as a drug target in COVID-19 [10]. In our earlier attempts we found out that penicillin's had the potential to bind to M^{pro} consistently, while phenoxymethylpenicillin and carbenicillin had high potential to act as an anti-COVID-19 agent which can be used alongside with anti-viral agents [11]. In another study, we repurposed USFDA approved drugs like aprepitant, barnidipine, tipiracil, arbutin and terbutaline by determining their binding ability to M^{pro} there by acting an anti-COVID-19 agents [12]. In the present study, we hypothesised that targeting multiple families of proteins of COVID-19 pathogenesis will have advantageous over the current approach. The molecular docking studies, induced fit docking, MM-GBSA followed by MD studies were performed for the selected class of antiviral, anti-inflammatory and immunomodulatory drugs such as chloroquine, hydroxychloroquine, lopinavir, ritonavir, remdesivir, ribavirin, arbidol, favipiravir, darunavir, oseltamivir, azithromycin, tetracycline, teicoplanin, sirolimus, baricitinib, cyclosporine, ivermectin, dexamethasone, nintedanib, resveratrol, quercetin, epigallocatechin 3-gallate betamethasone sodium phosphate, curcumin, andrographolide, nafamostat, camostat, nitazoxanide and fluvoxamine as ligands by considering the S-protein, ACE-2 and M^{pro} as proteins for all the studies.

Materials And Methods

Computational tools and study design

The protein crystal structures were downloaded from the proteins data bank (PDB) and UniProt, while the structures of ligands were taken from PubChem. Maestro Molecular modelling platform (Schrödinger, LLC, New York) was used for performing molecular docking studies followed by Induced fit docking, Prime MM-GBSA and MD simulations using Schrodinger software. Molecular docking was used to study the molecular interaction and binding affinity between the selected molecules and the target proteins which indicates the behaviour of the ligands (drugs/molecules) at the target protein site and to elucidate the underlying molecular mechanism. Then Prime MM-GBSA calculations followed by Induced Fit Docking. Top hit molecules were then subjected to MD simulation to evaluate the binding stability of the ligand on the target protein.

Selection of Suitable Protein Targets

Based on the literature, there are three important protein families who are involved in the pathogenesis of COVID-19, which includes ACE-2 (PDB ID: 6M1D), M^{pro} (PDB ID: 5R82) and spike protein (PDB ID: 1ZV8). The crystal structure of each protein was selected based on its resolution from PDB (http://www.rcsb.org/).

Preparation of Ligands

In this study antiviral, anti-inflammatory and immunomodulatory molecules were selected from the literature based on their mechanism of action as given in Table 1. The ligands structure was downloaded and incorporated into Maestro. Ligands were then optimized using LigPrep tool of Schrödinger (LigPrep, Schrödinger, LLC, New York, NY, 2020) to obtain appropriate geometry optimized stable structures with the lowest energy at neutral pH 7.0 [13].

Protein Preparation

The protein crystal structure was processed with Epik Protein Preparation Wizard (Schrödinger, LLC, New York, NY, 2020) where missing hydrogens, amino acid residues, and side chains were added. Proper ionization state for protein residues was generated, the water molecules were removed, and H-bond network was generated. The protein structure was energy minimized using the OPLS3 force field [37].

SiteMap

The SiteMap tool was used to identify druggable ligand-binding pocket in the proteins which lacks a bound ligand in its crystal structure, so as to identify the potential binding site for the ligand. SiteMap

module returns potential sites on the protein which are ranked based on their SiteScore and DScore. Based on these values, a binding site was selected, and the ligands were docked on the proteins [38].

Molecular Docking

The Glide module was used for performing molecular docking. Receptor grid was generated using the receptor grid generation tool which defines the region on the protein onto which the module needs to introduce the ligands for docking. After the generation of receptor grid, grid file was loaded, and prepared ligands were selected from the table, docking was performed in extra precision (XP) mode. The docked ligand poses were then analysed for the interaction pattern with the protein; the ligand pose with the best interaction with the protein was selected. The top hits obtained from molecular docking was selected and subjected to induce fit docking, prime MM-GBSA and MD simulations [39].

Prime MM-GBSA

The MM-GBSA was used to determine the ligand binding energies and ligand strain energies for the top hits in docking studies. Prime MM-GBSA module of Schrödinger was employed for this purpose. OPLS3e force field was used with VSGB solvent model, while the ligands and receptor are taken from the project table and workspace respectively. As the MM-GBSA binding energies are approximate free energies of binding, a more negative value indicates stronger binding (reported in kcal/mol).

Induced Fit Docking

Induced fit docking (IFD) protocol was carried out using the induced-fit tool in Maestro (Induced Fit Docking Schrödinger, LLC, New York, NY, 2020) on the selected proteins with the top hits obtained from docking studies and prime MM-GBSA. The prime reason for performing IFD, is to permit flexibility to both ligand and protein, which is restricted in docking studies. IFD is reported to be robust and accurate in predicting the binding affinity between the ligand and the protein pocket of the protein. Ligand docking and protein refinement are carried out using glide and prime, respectively in IFD tool.

Molecular Dynamics (MD) Simulation

MD simulation was performed for the shortlisted molecules from the results of IFD and MM-GBSA using the Desmond module (Desmond Molecular Dynamics System, New York, NY, 2020). Initially, the solvated complex system was prepared using TIP3P as a predefined solvent model, and the iso-osmotic condition was maintained in this stage. The System Builder module was used for the preparation of the above system. The solvated system was minimized using the Minimization module. It was then loaded and minimized using the 2000 maximum iterations and 1.0 (kcal/mol/Å) convergence threshold. The minimized solvated system was used for running the MD simulation. MD simulation was performed with NPT ensemble for 100 ns at 1.01 bar pressure and 300K temperature. MD simulation results of all ligands were analysed by generating the simulation interaction diagram [40].

Results

Molecular docking, Prime MM-GBSA and Induced fit docking

Molecular docking was performed on the protein main protease (M^{pro}, PDB ID: 5R82) with known binding site whereas SiteMap was performed for the proteins which in their crystal structure lacked a bound ligand, due to which the binding site is not clearly known (ACE2 and spike protein, PDB ID: 6M1D and 1ZV8, respectively). SiteMap helps in identifying the druggable binding site on the protein, based on analysis of the entire protein. The results of the SiteMap analysis were obtained as Site-score and D-score (Table 2). On the basis of SiteMap analysis results, for 1ZV8 protein, Site-1 showed highest Site-Score (1.022) as well as D-Score (1.037) whereas for 6M1D protein, Site-5 showed highest Site-Score (1.11) and D-score (1.162). Thus, these sites were selected for performing the molecular docking studies. Table 3 summarises the docking score, IFD score and ΔG values for the three proteins and Fig. 1 shows the 2D ligand interaction diagrams between the ligands and the proteins, in protein 6M1D site-5 nintedanib has highest docking score (-6.056) and ΔG value (-44.53) while baricitinib followed closely behind with a docking score (-5.76) and ΔG value (-40.66) and ivermectin showed the least docking score (-5.328) and ΔG value (-17.33). Nintedanib formed π-cation interaction with LYS454, π-π stacking interaction with PHE497 and H-bonds with MET460 while baricitinib formed H-bonds with THR9 (Fig. 1 A and B). In case of protein 5R82, nintedanib has highest docking score (-5.428) and ΔG value (-50.42), but IFD score (-643.67) was less when compared with darunavir which showed a docking score (-4.691), ΔG value (-47.691) and IFD score (-649.42). Fluvoxamine and favipiravir showed docking score (-4.631 & -3.968) and Δ G value (-42.4 & -23.42), fluvoxamine showed the least IFD score (-641.05), but compared to nintedanib, the favipiravir showed a better IFD score (-643.92). Nintedanib formed π-π stacking interactions with HIE41 and H-bonds with SER46 while darunavir showed π-π stacking interactions with HIE41 and H-bonds with ASN142 and GLN189 amino acid residues (Fig. 1C and 1D). Finally, for 1ZV8 Site-1 it is seen that quercetin showed highest docking score (-4.958) and IFD score (-1181.47), but nintedanib showed highest prime MM-GBSA score (ΔG value =-40) while having a docking score (-4.113) and IFD score (-1172.72) close to that of quercetin. Lopinavir and hydroxychloroquine showed a docking score (-3.521 and -3.464) and prime MM-GBSA (ΔG -35.61 and -24.44). However, lopinavir has marginally better IFD score (-1175.01) than that of nintedanib, whereas hydroxychloroquine showed the least IFD score (-1172.02). Nintedanib exhibits amino acid interactions such as π-cation interactions and H-bonds with LYS24. In addition to this, it also formed H-bonds with SER14 and GLU18. In comparison, quercetin formed H-bonds with ASP32, THR25 and GLU18 (Fig. 1 E and F).

Molecular Dynamics (MD) Simulation

After performing the initial computational studies, binding mode stability of the selected molecules on the different proteins were analyzed by MD simulation studies. The simulation interaction diagram shows us various parameters like protein root mean square deviations (RMSD), ligand RMSD, protein root mean square fluctuation (RMSF), ligand RMSF and interactions observed between the ligand and the amino acids of the protein among other results. It can be seen from Fig. 2A and 2B the P-RMSD and L-RMSD of

nintedanib and baricitinib on 6MID respectively, in Fig. 2A, the two plots are fairly close to one another which indicates that the ligand-protein complex did not get disassociated at any time during the 100 nsec simulation and the RMSD difference are between 2.5Å while baricitinib (Fig. 2B), when complexed with the protein seems to be dissociated up until 60 nsec after which shows a stable presence in the protein binding pocket with an RMSD difference within 2.5 Å. Fig 2 C and D shows the P-RMSD and L-RMSD of nintedanib and darunavir on 5R82 respectively, and it can be seen that nintedanib after 40 ns of simulation separates away from the protein binding pocket. This disassociation is also reflected in the RMSD value which is more than 2.5 Å while darunavir, on the other hand, shows a very stable binding interaction with the protein with an RMSD difference well within 2.5Å. L-RMSD and P-RMSD represented in Fig 2. E and F are of nintedanib and quercetin on 1ZV8, respectively. It can be seen that Nintedanib shows a stable binding with the protein from 30 to 40 ns and then from 70 to 90 ns with an RMSD difference less than 2.5 Å while quercetin showed a stable binding interaction with the protein binding pocket from 50 to 100 ns with an RMSD difference well within 2.5Å. Along with RMSDs it is also important to have an idea about the intermolecular interactions being formed between the ligand and the protein such as H-bonds, hydrophobic interactions, π-π stacking, π-cation, salt bridges, water bridges. These can be graphically visualized by protein-ligand contacts plot through a bar diagram and are reported in fraction interaction (in %). Fig 3. represents the protein-ligand contacts seen between the ligands and the proteins. Interactions between nintedanib and baricitinib with 6M1D are represented in Fig. 3A and 3B respectively, nintedanib forms H-bonds with MET460 for 78% while forming hydrophobic bonds with PHE 453 and 497 at 85.3% and 57.6% respectively, it also forms water bridge interactions with HIS446 at 79%, LEU489 at 39.8%, PHE457 at 48.3% and GLY492 at 29.1% whereas baricitinib forms H-bonds with MET460 at 58.2%, GLN465 at 35.7% and GLN13 at 27.3%. Baricitinib forms hydrophobic bonds with PHE 453 and 497 at 47.7% and 46.8% respectively while showing water bridge interactions with LYS11 at 47.9%. The protein-ligand contacts exhibited in Fig. 3C and 3D are of nintedanib and darunavir on 5R82, respectively. It can be seen that darunavir forms H-bonds at 42.8% with GLN189 while forming hydrophobic bonds with HIS41 at 68.3%, MET49 at 38.2% and with MET165 at 29.5%. Darunavir forms water bridge interactions with THR26 at 39%, GLY14 at 35.5%, CYS145 at 60.5% and with GL166 at 102% whereas nintedanib forms H-bonds with THR26 and SER46 at 37.4% and 50.7% respectively. Hydrophobic bonds are formed with HIS41 at 72.5%, MET49 at 59.1% and with MET165 at 43.5% while showing water bridge interactions with HIS164 and GLU166 at 40.2% and 64.9%. Finally, Fig. 3E and 3F represent the protein-ligand contacts between nintedanib and quercetin with 1ZV8 respectively, nintedanib forms H-bonds with GLU18 and SER14 at 98.8% and 89.7% respectively while forming water bridge interaction with THR25 at 36.7% whereas, quercetin forms H-bonds with ASP32 at 43.8%, ASN20 at 90.4% and with GLU18 at 28.5% while forming water bridge interactions with LYS24 and SER14 at 39.7% and 27.4%. Similar to PL contacts there are ligand-protein (LP) contacts which have been mentioned in table 4. Additionally, P-RMSF was calculated and illustrated in Fig. 4 each peak corresponds to the region of protein that has fluctuated, usually the N and C terminals of the protein fluctuates the most. Fig. 4A and 4B represent the P-RMSF when nintedanib and baricitinib are complexed with 6M1D, and it can be seen that the protein fluctuates less when baricitinib is complexed with it while in case of 5R82 (Fig. 4C and 4D) the presence of nintedanib and darunavir have rendered the protein equally

fluctuated. Fig. 4E and 4F indicates the P-RMSF of 1ZV8 when complexed with nintedanib and quercetin respectively, and it can be seen that when complexed with nintedanib, the protein is less fluctuated.

Similar to protein RMSF, Fig. 5 illustrates the ligand RMSF and shows the atoms in the ligand that show the highest fluctuation. For nintedanib, the atoms that show most fluctuations are 10, 37, 38 and 40 across all three proteins. Fig. 5B represent the L-RMSF of baricitinib on 6M1D, the atoms that fluctuate the most are atom 3, 4 and 5. L-RMSF of darunavir on 5R82 is represented by Fig. 5D, and it can be seen that atoms 18, 19, 22, 27, 28, 29, 30 and 31 fluctuate the most. The L-RMSF of quercetin on 1ZV8 is shown in Fig. 5F, the atoms that fluctuate the most are 10, 17, 18, 19, 20, 21 and 22. Fig. 6 represents the 3D conformation of the ligand when it occupies the protein pocket, the dotted lines depict the amino acid interactions.

Discussion

A considerable number of computational docking and predictions for treatment of COVID-19 are in progress. The success of repurposed drugs such as remdesivir, favipiravir and dexamethasone are the stimulus for further computational predictions. In the current approach, the computationally repurposed drugs are further screened for multiple targets, and the suitable one was proposed for COVID-19 therapy. The ligands selected from the literature survey were initially subjected to molecular docking studies, the ligand which showed the highest docking score along with good amino acid interactions are then checked for prime MM-GBSA and IFD. Prime MM-GBSA score is represented by ΔG and is indicative of the energy changes involved when a ligand tries to occupy the binding site of a protein. The higher energy spent the less chance of it to disassociate from that binding site. For all these three parameters, a greater negative value is indicative of higher strength. For protein 6M1D, nintedanib is showing the best docking score and ΔG value which is followed by baricitinib, the amino acid interactions are also greater in number for nintedanib. The other ligands underperformed and showed poor amino acid interactions with 6M1D due to which nintedanib and baricitinib were selected for MD simulation. In case of protein, 5R82-nintedanib had higher docking score and ΔG value, but darunavir had greater IFD score, Fluvoxamine and favipiravir when compared had lesser docking score and ΔG than that for nintedanib and darunavir. However, based on the amino acid interactions, it was evident that darunavir has more interactions than nintedanib while fluvoxamine and favipiravir showed less interactions. This was the reason why nintedanib and darunavir were selected for MD simulation as they out-performed the other ligands. Finally, for protein 1ZV8-quercetin exhibited the highest docking score and IFD score while nintedanib had greater ΔG value. Lopinavir and hydroxychloroquine lower docking score but lopinavir had an IFD score which was greater than nintedanib and ΔG value greater than quercetin. Upon inspecting amino acid interactions, it was clear that nintedanib showed more interactions which was followed by quercetin while lopinavir and hydroxychloroquine had less interactions. Hence quercetin and nintedanib were selected for MD simulation.

MD simulation studies help in understanding the behavior of docked ligand on the protein in a solvated system over a period of time under simulated biological conditions. For protein 6M1D it was seen that

nintedanib and baricitinib showed RMSD value within 2.5 Å. The RMSD plots show that nintedanib is staying in the protein binding pocket which can be understood from Fig. 2A the two lines are fairly overlapping for most of the time whereas, it can be seen that the two lines are farther away from each other in Fig. 2B indicating that baricitinib initially separates out from the protein pocket later sitting in it. When protein-ligand contacts are measured it can be seen that nintedanib has a greater number of interactions crossing the 50% mark with amino acids (Fig. 3A and 3B) than what is shown by baricitinib. This increased number of interactions with the protein might be the reason why nintedanib is staying in the protein binding pocket, but baricitinib is not. Although the P-RMSF (Fig. 4A and 4B) and L-RMSF (Fig. 5A and 5B) seem to be slightly better for baricitinib, with less protein fluctuations when baricitinib is complexed, it is not superior to nintedanib as the difference is not much. Based on these results, it is clear that for 6M1D-nintedanib is showing better affinity amongst all the ligands. In the case of protein 5R82, from RMSD plot (Fig. 2D) it is clear that darunavir is staying in the protein binding pocket for the entire simulation period while nintedanib is not (Fig. 2C). The RMSD value is greater than 2.5 Å for nintedanib but not for darunavir. A similar trend is being seen in the case of protein-ligand contacts (Fig. 3C and 3D), darunavir has a greater number of interactions with amino acid when compared with nintedanib. P-RMSF (Fig. 4C and 4D) is the same for both the proteins indicating that the presence of ligand has fluctuated the protein equally while L-RMSF (Fig. 5C and 5D) is better for darunavir. From the results, it is understood that for protein 5R82 darunavir is showing better affinity while nintedanib follows closely behind. Finally, for protein 1ZV8 nintedanib and quercetin show an RMSD value within 2.5 Å and both the ligand do not occupy the protein binding pocket for the entire duration of the simulation (Fig. 2E and 2F). The amino acid interaction between the ligand and protein was seen to be equal for both nintedanib and quercetin (Fig. 3E and 3F), but nintedanib showed interactions of better quality and stability. P-RMSF plot reveals that when complexed with nintedanib, the protein seems to be less fluctuated when compared with quercetin (Fig. 4E and 4F) while L-RMSF (Fig. 5E and 5F) shows nintedanib is less fluctuated when compared with quercetin. From these, it can be stated that for protein 1ZV8 nintedanib shows better affinity. From the MD results it can be concluded that across all three proteins, nintedanib can be selected as a ligand for multi-targeting as it shows superior affinity with all three proteins when compared with rest of the proteins.

Currently, COVID-19 management options are supportive therapy, preventive control measures in hospital settings. It takes a great deal of time for USFDA to receive and approve drugs specific to SARS-CoV-2 due to which researches resort to repurpose existing approved molecules for the management of COVID-19. Drugs such as favipiravir, nelfinavir, ivermectin, lopinavir, remdesivir, baricitinib and tocilizumab are being tested clinically to evaluate their effectiveness against SARS-CoV-2 [7]. Though the drug remdesivir is approved to be the drug for COVID-19, there are limitations for the use effectively in most of the patients [41]. The route of administration of remdesivir also is concern for effective management of COID-19 [42]. All these attempts are focused on a single family of protein in SARS-CoV-2, but in actuality, there are more than one prominent family of protein playing a major role in the functioning of SARS-CoV-2. In this drug repurposing study, we focused on three major family of proteins and tried to identify one drug molecule which can bind to all three proteins thereby enabling multi targeting. A single molecule having the ability

to interact with the three proteins which will result in better efficacy. Of the molecules selected nintedanib, quercetin, darunavir and baricitinib showed the most promising interactions with the three proteins across molecular docking, induced-fit docking, prime MM-GBSA and molecular dynamic simulations. The molecular docking score (-4.113), δG value (-40) and IFD (-1172.72) score of nintedanib was superior to the remaining selected drugs, which was closely followed by quercetin for 1ZV8 protein. In the case of 5R82 protein, nintedanib has highest docking score (-5.482) and δG (-50.42), but the IFD score (-643.67) was less when compared with darunavir. For 6M1D protein, nintedanib showed highest docking score (-6.056) and δG value (-44.53). In MD simulation of nintedanib, after 40 nsec of simulation separates away from the 5R82 respectively protein binding pocket, whereas it was stable with 1ZV8 and 6M1D proteins. Nintedanib is used in the treatment of various lung diseases like idiopathic pulmonary fibrosis (IPF), systemic sclerosis-associated interstitial lung disease and non-small cell lung cancer along with docetaxel [43]. It is found to reduce the incidence of acute exacerbation of IPF in COVID-19 patients. It was reported that repurposing of nintedanib had been beneficial for the treatment of COVID-19 patients to treat severe lung fibrosis. Clinical trials (phase-II) are going on nintedanib to check the safety and efficacy to treat idiopathic pulmonary fibrosis in COVID-19 patients [44]. The pathophysiological similarities that exist between IPF and COVID-19 suggest that the pathogenic mechanism that leads to pulmonary fibrosis in these two conditions are same, hence it makes sense to use drugs used in case of IPF to manage COVID-19. Nintedanib is one such kinase inhibitor which has affinity to viral protein and shows its action on pulmonary proteins as well. The use of antifibrotic agents make sense in case of COVID-19 because the occurrence of pulmonary fibrotic disease after COVID-19 recovery is seen.

Conclusion

Based on the results of molecular docking score, ΔG value and IFD score, two best molecules were selected, based on the stable molecular interactions. Nintedanib, quercetin, darunavir and baricitinib were shortlisted and the most preferred interaction was seen in nintedanib in MD simulation with spike proteins, M^{pro} and 6M1D proteins. Thus nintedanib could be the suitable molecule for the treatment of COVID-19, but it needs to be validated experimentally and clinically.

Declarations

Funding: Authors are thankful to the support from Manipal Academy of Higher Education, Manipal, India for TMA Pai Fellowship to Varalakshmi Velagacherla and Akhil Suresh. Authors also thankful to DST-SERB grant for Computer simulations Schrodinger's Suit Software (#EMR/2016/007006)

Conflict of interest: The authors declare that they have no conflict of interest.

Author contributions: UYN and YN: Concept and idea for design of hypothesis, guided the computational experiments, final approval and correction of the version to be published. VV, AS and CHM: Execution of computational experiments, results generation and compilation, manuscript drafting and revisions.

References

[1] Zhu N, Zhang D, Wang W, Li X, Yang B, Song J, et al. A novel coronavirus from patients with pneumonia in China, 2019. New England Journal of Medicine 2020;382:727–33. https://doi.org/10.1056/NEJMoa2001017.

[2] Shereen MA, Khan S, Kazmi A, Bashir N, Siddique R. COVID-19 infection: Origin, transmission, and characteristics of human coronaviruses. Journal of Advanced Research 2020;24:91–8. https://doi.org/10.1016/j.jare.2020.03.005.

[3] Lovato A, de Filippis C. Clinical Presentation of COVID-19: A Systematic Review Focusing on Upper Airway Symptoms. Ear, Nose and Throat Journal 2020. https://doi.org/10.1177/0145561320920762.

[4] Mason RJ. Pathogenesis of COVID-19 from a cell biology perspective. European Respiratory Journal 2020;55:2000607. https://doi.org/10.1183/13993003.00607-2020.

[5] Guo Y-R, Cao Q-D, Hong Z-S, Tan Y-Y, Chen S-D, Jin H-J, et al. The origin, transmission and clinical therapies on coronavirus disease 2019 (COVID-19) outbreak- A n update on the status. Military Medical Research 2020;7:1–10. https://doi.org/10.1186/s40779-020-00240-0.

[6] Naqvi AAT, Fatima K, Mohammad T, Fatima U, Singh IK, Singh A, et al. Insights into SARS-CoV-2 genome, structure, evolution, pathogenesis and therapies: Structural genomics approach. Biochimica et Biophysica Acta (BBA) - Molecular Basis of Disease 2020;1866:165878. https://doi.org/10.1016/j.bbadis.2020.165878.

[7] Barlow A, Landolf KM, Barlow B, Yeung SYA, Heavner JJ, Claassen CW, et al. Review of Emerging Pharmacotherapy for the Treatment of Coronavirus Disease 2019. Pharmacotherapy 2020;40:416–37. https://doi.org/10.1002/phar.2398.

[8] Sanders JM, Monogue ML, Jodlowski TZ, Cutrell JB. Pharmacologic Treatments for Coronavirus Disease 2019 (COVID-19): A Review. JAMA - Journal of the American Medical Association 2020;323:1824–36. https://doi.org/10.1001/jama.2020.6019.

[9] Elfiky AA. Anti-HCV, nucleotide inhibitors, repurposing against COVID-19. Life Sciences 2020;248. https://doi.org/10.1016/j.lfs.2020.117477.

[10] Sahu K, Noskov S, Tuszynski J, Houghton M, Tyrrell L. Computational Screening of Molecules Approved in Phase-I Clinical Trials to Identify 3CL Protease Inhibitors to Treat COVID-19. 2020. https://doi.org/10.20944/preprints202004.0015.v2.

[11] Krishnaprasad B, Maity S, Mehta C, Suresh A, Nayak UY, Nayak Y. In Silico Drug Repurposing of Penicillins to Target Major Protease Mpro of SARS-CoV-2. Pharmaceutical Sciences 2020. https://doi.org/10.34172/PS.2020.44.

[12] Baby K, Maity S, Mehta CH, Suresh A, Nayak UY, Nayak Y. Targeting SARS-CoV-2 Main Protease: A Computational Drug Repurposing Study. Archives of Medical Research 2020. https://doi.org/10.1016/j.arcmed.2020.09.013.

[13] Chen I-J, Foloppe N. Drug-like bioactive structures and conformational coverage with the ligprep/confgen suite: Comparison to programs MOE and catalyst. Journal of Chemical Information and Modeling 2010;50:822–39. https://doi.org/10.1021/ci100026x.

[14] Yang C, Ke C, Yue D, Li W, Hu Z, Liu W, et al. Effectiveness of Arbidol for COVID-19 Prevention in Health Professionals. Frontiers in Public Health 2020;8. https://doi.org/10.3389/fpubh.2020.00249.

[15] Kelleni MT. Nitazoxanide/azithromycin combination for COVID-19: A suggested new protocol for early management. Pharmacological Research 2020;157. https://doi.org/10.1016/j.phrs.2020.104874.

[16] Enmozhi SK, Raja K, Sebastine I, Joseph J. Andrographolide as a potential inhibitor of SARS-CoV-2 main protease: an in silico approach. Journal of Biomolecular Structure & Dynamics 2020:1–7. https://doi.org/10.1080/07391102.2020.1760136.

[17] Zhang R, Wang X, Ni L, Di X, Ma B, Niu S, et al. In silico studies on therapeutic agents for COVID-19: Drug repurposing approach. Life Sciences 2020;248. https://doi.org/10.1016/j.lfs.2020.117592.

[18] Lammers T, Sofias AM, van der Meel R, Schiffelers R, Storm G, Tacke F, et al. Dexamethasone nanomedicines for COVID-19. Nature Nanotechnology 2020;15:622–4. https://doi.org/10.1038/s41565-020-0752-z.

[19] Hou Y, Zhao J, Martin W, Kallianpur A, Chung MK, Jehi L, et al. New insights into genetic susceptibility of COVID-19: An ACE2 and TMPRSS2 polymorphism analysis. BMC Medicine 2020;18. https://doi.org/10.1186/s12916-020-01673-z.

[20] Meyerowitz EA, Vannier AGL, Friesen MGN, Schoenfeld S, Gelfand JA, Callahan M V, et al. Rethinking the role of hydroxychloroquine in the treatment of COVID-19. FASEB Journal 2020;34:6027–37. https://doi.org/10.1096/fj.202000919.

[21] Zahedipour F, Hosseini SA, Sathyapalan T, Majeed M, Jamialahmadi T, Al-Rasadi K, et al. Potential effects of curcumin in the treatment of COVID-19 infection. Phytotherapy Research 2020:ptr.6738. https://doi.org/10.1002/ptr.6738.

[22] de Wilde AH, Zevenhoven-Dobbe JC, van der Meer Y, Thiel V, Narayanan K, Makino S, et al. Cyclosporin A inhibits the replication of diverse coronaviruses. The Journal of General Virology 2011;92:2542–8. https://doi.org/10.1099/vir.0.034983-0.

[23] Sang P, Tian S-H, Meng Z-H, Yang L-Q. Anti-HIV drug repurposing against SARS-CoV-2. RSC Advances 2020;10:15775–83. https://doi.org/10.1039/d0ra01899f.

[24] Marinella MA. Routine antiemetic prophylaxis with dexamethasone during COVID-19: Should oncologists reconsider? Journal of Oncology Pharmacy Practice 2020. https://doi.org/10.1177/1078155220931921.

[25] Menegazzi M, Campagnari R, Bertoldi M, Crupi R, Di Paola R, Cuzzocrea S. Protective Effect of Epigallocatechin-3-Gallate (EGCG) in Diseases with Uncontrolled Immune Activation: Could Such a Scenario Be Helpful to Counteract COVID-19? International Journal of Molecular Sciences 2020;21:5171. https://doi.org/10.3390/ijms21145171.

[26] Neogi U, Hill KJ, Ambikan AT, Heng X, Quinn TP, Byrareddy SN, et al. Feasibility of known rna polymerase inhibitors as anti-sars-cov-2 drugs. Pathogens 2020;9. https://doi.org/10.3390/pathogens9050320.

[27] García IG, García IG, Rodriguez-Rubio M, Rodriguez-Rubio M, Mariblanca AR, Mariblanca AR, et al. A randomized multicenter clinical trial to evaluate the efficacy of melatonin in the prophylaxis of SARS-CoV-2 infection in high-risk contacts (MeCOVID Trial): A structured summary of a study protocol for a randomised controlled trial. Trials 2020;21. https://doi.org/10.1186/s13063-020-04436-6.

[28] Zeitlinger M, Koch BCP, Bruggemann R, De Cock P, Felton T, Hites M, et al. Pharmacokinetics/Pharmacodynamics of Antiviral Agents Used to Treat SARS-CoV-2 and Their Potential Interaction with Drugs and Other Supportive Measures: A Comprehensive Review by the PK/PD of Anti-Infectives Study Group of the European Society of Antimicr. Clinical Pharmacokinetics 2020. https://doi.org/10.1007/s40262-020-00924-9.

[29] Choudhary R, Sharma AK. Potential use of hydroxychloroquine, ivermectin and azithromycin drugs in fighting COVID-19: trends, scope and relevance. New Microbes and New Infections 2020;35. https://doi.org/10.1016/j.nmni.2020.100684.

[30] Bhatnagar T, Murhekar M, Soneja M, Gupta N, Giri S, Wig N, et al. Lopinavir/ritonavir combination therapy amongst symptomatic coronavirus disease 2019 patients in India: Protocol for restricted public health emergency use. Indian Journal of Medical Research 2020;151:184–9. https://doi.org/10.4103/ijmr.IJMR_502_20.

[31] Hifumi T, Isokawa S, Otani N, Ishimatsu S. Adverse events associated with nafamostat mesylate and favipiravir treatment in COVID-19 patients. Critical Care 2020;24. https://doi.org/10.1186/s13054-020-03227-4.

[32] Shiratori T, Tanaka H, Tabe C, Tsuchiya J, Ishioka Y, Itoga M, et al. Effect of nintedanib on non-small cell lung cancer in a patient with idiopathic pulmonary fibrosis: {A} case report and literature review. Thoracic Cancer 2020;11:1720–3. https://doi.org/10.1111/1759-7714.13437.

[33] Maurya VK, Kumar S, Prasad AK, Bhatt MLB, Saxena SK. Structure-based drug designing for potential antiviral activity of selected natural products from Ayurveda against SARS-CoV-2 spike

glycoprotein and its cellular receptor. VirusDisease 2020. https://doi.org/10.1007/s13337-020-00598-8.

[34] Zhavoronkov A. Geroprotective and senoremediative strategies to reduce the comorbidity, infection rates, severity, and lethality in gerophilic and gerolavic infections. Aging 2020;12:6492–510. https://doi.org/10.18632/aging.102988.

[35] Baron SA, Devaux C, Colson P, Raoult D, Rolain J-M. Teicoplanin: an alternative drug for the treatment of COVID-19? International Journal of Antimicrobial Agents 2020. https://doi.org/10.1016/j.ijantimicag.2020.105944.

[36] Bharadwaj S, Lee KE, Dwivedi VD, Kang SG. Computational insights into tetracyclines as inhibitors against SARS-CoV-2 Mpro via combinatorial molecular simulation calculations. Life Sciences 2020;257. https://doi.org/10.1016/j.lfs.2020.118080.

[37] Roos K, Wu C, Damm W, Reboul M, Stevenson JM, Lu C, et al. OPLS3e: Extending Force Field Coverage for Drug-Like Small Molecules. Journal of Chemical Theory and Computation 2019;15:1863–74. https://doi.org/10.1021/acs.jctc.8b01026.

[38] Halgren TA. Identifying and Characterizing Binding Sites and Assessing {Druggability}. Journal of Chemical Information and Modeling 2009;49:377–89. https://doi.org/10.1021/ci800324m.

[39] Friesner RA, Murphy RB, Repasky MP, Frye LL, Greenwood JR, Halgren TA, et al. Extra precision glide: docking and scoring incorporating a model of hydrophobic enclosure for protein-ligand complexes. Journal of Medicinal Chemistry 2006;49:6177–96. https://doi.org/10.1021/jm051256o.

[40] Bowers KJ, Chow E, Xu H, Dror RO, Eastwood MP, Gregersen BA, et al. Scalable algorithms for molecular dynamics simulations on commodity clusters. Proceedings of the 2006 ACM/IEEE Conference on Supercomputing, SC'06 2006. https://doi.org/10.1145/1188455.1188544.

[41] Wang Y, Zhang D, Du G, Du R, Zhao J, Jin Y, et al. Remdesivir in adults with severe COVID-19: a randomised, double-blind, placebo-controlled, multicentre trial. The Lancet 2020;395:1569–78. https://doi.org/10.1016/S0140-6736(20)31022-9.

[42] Sun D. Remdesivir for Treatment of COVID-19: Combination of Pulmonary and IV Administration May Offer Aditional Benefit. AAPS Journal 2020;22. https://doi.org/10.1208/s12248-020-00459-8.

[43] Rivera-Ortega P, Hayton C, Blaikley J, Leonard C, Chaudhuri N. Nintedanib in the management of idiopathic pulmonary fibrosis: clinical trial evidence and real-world experience. Therapeutic Advances in Respiratory Disease 2018;12. https://doi.org/10.1177/1753466618800618.

[44] Zhang C, Li J, Wu Z, Wang H, Que C, Zhao H, et al. Efficacy and safety of anluohuaxian in the treatment of patients with severe coronavirus disease 2019- a multicenter, open label, randomized controlled study: A structured summary of a study protocol for a randomised controlled trial. Trials 2020;21. https://doi.org/10.1186/s13063-020-04399-8.

Tables

Table 1. List of ligands selected for computational studies

Drug Name	Category of Drug	MOA on SARS-COV2	References
Arbidol	Anti-viral	Interacts with viral lipid envelope and clathrin mediated endocytosis	[14]
Azithromycin	Antibiotic	By increasing endosomal pH and inhibiting replication of virus	[15]
Andrographolide	Anti-viral and anti-inflammatory	Inhibits SARS-Co-V M^{pro} /$3CL^{pro}$	[16]
Baricitinib	Immunosuppressant	By inhibiting Janus kinase	[17]
Betamethasone sodium phosphate	Corticosteroid, immunomodulatory	Inhibits synthesis of inflammatory mediators	[18]
Camostat	Serine protease inhibitor, in Pancreatitis	Inhibits TMPRSS2 protein	[19]
Chloroquine	Anti-malarial	Increasing endosomal pH	[20]
Curcumin	Polyphenol (anti-viral), anti-inflammatory	Prevents entry of the virus into host cells and inhibits SARS-Co-V protease	[21]
Cyclosporine	Immunosuppressant	By inhibition of RdRp	[22]
Darunavir	Anti-viral	By protease inhibition	[23]
Dexamethasone	Corticosteroid, immunomodulatory	Alters inflammatory agents and immune responses	[24]
Epigallocatechin-3 gallate	Flavonoid, anti-inflammatory	Inhibits SARS-Co-v M^{pro} /$3CL^{pro}$	[25]
Favipiravir	Ant-viral	Inhibits RdRp	[26]
Fluvoxamine	Anti-depressant	Inhibits viral M^{pro} /$3CL^{pro}$	[27]
Hydroxy chloroquine	Anti-malarial	Interaction with ACE-2 and glycosylation	[28]
Ivermectin	Anthelmintic	Inhibits replication of virus	[29]
Lopinavir & ritonavir	Antiviral	Inhibition of M^{pro} /$3CL^{pro}$	[30]
Nafamostat	Serine protease inhibitor in pancreatitis	Inhibits TMPRSS2 protein	[31]
Nintedanib	Anti-fibrotic agent	By inhibiting tyrosine kinases	[32]
Nitazoxanide	Anti-protozoal and anti-viral	Inhibits production of pro-inflammatory cytokines	[15]

Oseltamivir	Anti-viral	Inhibits neuraminidase	[17]
Quercetin	Flavonoid, anti-inflammatory	Inhibits SARS-CoV M^{pro} /$3CL^{pro}$	[33]
Remdesivir	Anti-viral	Inhibits replication of virus	[17]
Resveratrol	Anti-viral, anti-inflammatory (Polyphenol)	Inhibits both replication of virus and synthesis of proteins	[33]
Ribavirin	Anti-viral	Prevents synthesis of mRNA-capping polymerase and replication of virus	[17]
Sirolimus	Immunosuppressant	By inhibiting mTOR signaling pathway	[34]
Teicoplanin	Antibiotic	Targets spike protein at cleavage site on cathepsin L	[35]
Tetracycline	Antibiotic	By forming complexes with zinc present in viral cellular components and decreases cytokine levels	[36]

Table 2. Site-score and D-score for the sites on 1ZV8 and 6M1D

Sites	Proteins			
	1ZV8		6M1D	
	Site-Score	D-Score	Site-Score	D-Score
Site-1	1.022	1.037	1.045	0.971
Site-2	0.92	0.932	1.032	1.026
Site-3	0.878	0.876	1.038	1.056
Site-4	0.978	0.929	1.107	1.043
Site-5	1.014	1.004	1.11	1.162

Table 3. Docking score, MM-GBSA and IFD-Score

Protein	Ligands	Docking Score	MM-GBSA	IFD -Score
6M1D	Nintedanib	-6.056	-44.32	-
	Baricitinib	-5.76	-40.66	-
	Ivermectin	-5.328	-17.33	-
5R82	Nintedanib	-5.482	-50.42	-643.67
	Darunavir	-4.691	-47.28	-649.44
	Fluvoxamine	-4.631	-42.4	-641.05
	Favipiravir	-3.698	-23.42	-643.92
1ZV8	Quercetin	-4.985	-35.45	-1181.47
	Nintedanib	-4.113	-40	-1172.72
	Lopinavir	-3.521	-35.61	-1175.01
	Hydroxychloroquine	-3.464	-24.44	-1172.02

Table 4. Ligand-protein contacts exhibited during MD simulation

Protein	Ligand	L-P Contacts %
5R82	**Darunavir**	34 (THR26)
		68 (HIS41)
		32 (GLY143)
		57 (CYS145)
		77 (GLU166)
		42 (GLN189)
	Nintedanib	72 (HIS41)
		31 (SER46)
		35 (HIS164)
		32 (GLU166)
6M1D	**Baricitinib**	31 (LYS11)
		58 (MET460)
		33 (GLN465)
	Nintedanib	35 (HIS446)
		35 (PHE453)
		44 (PHE457)
		78 (MET460)
		39 (LEU489)
1ZV8	**Nintedanib**	89 (SER14)
		98 (GLU18)
	Quercetin	46 (ASN20)
		38 (ASP32)

Figures

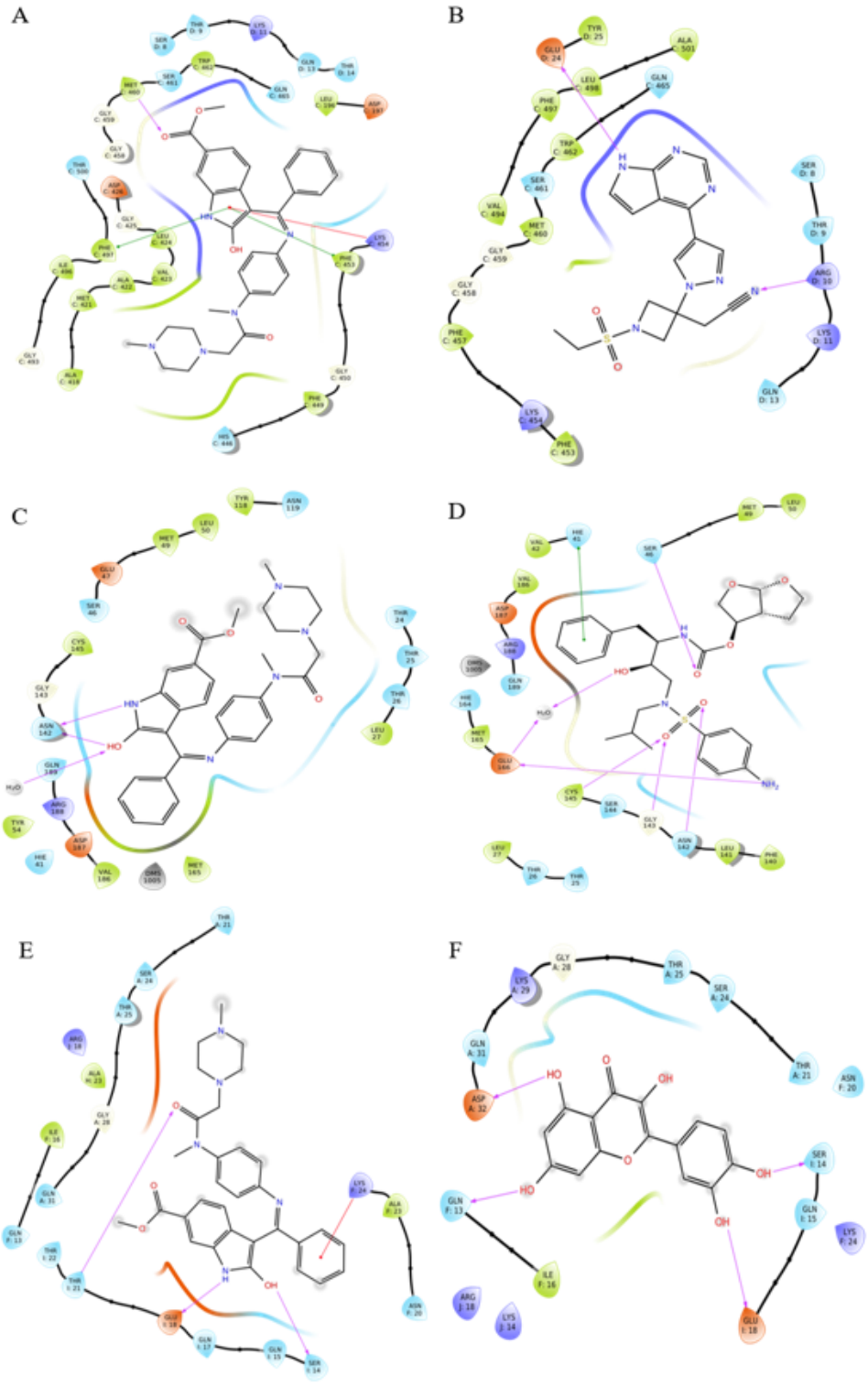

Figure 1

2D Ligand interaction diagram A: Nintedanib, B: Baricitinib on ACE2 Protein, PDBID: 6M1D; C: Nintedanib, D: Darunavir on Mpro, PDBID: 5R82; E: Nintedanib; F: Quercetin on Spike Protein. PDBID: 1ZV8

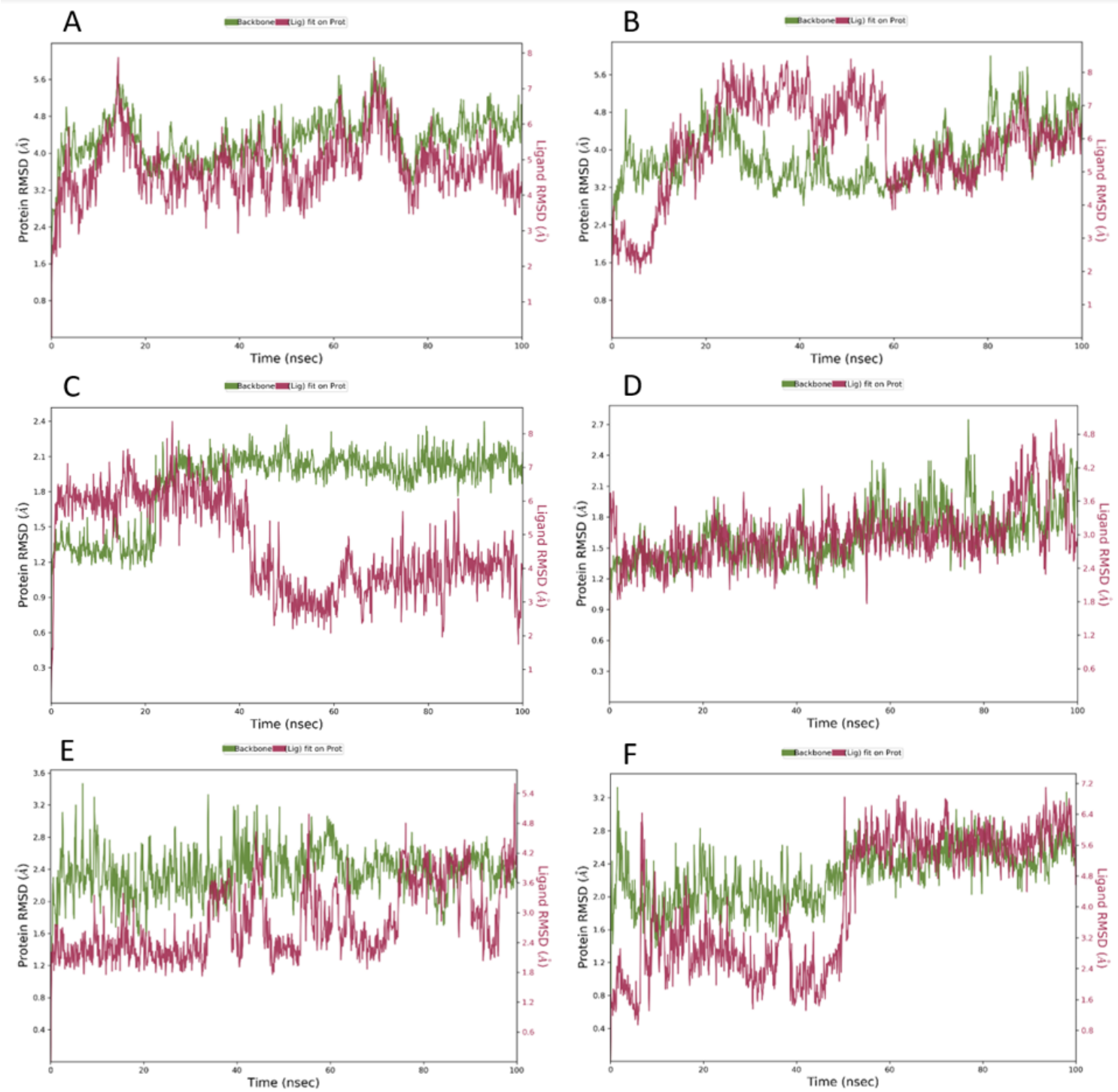

Figure 2

RMSD plot for ligand-protein interaction A: Nintedanib, B: Baricitinib on ACE2 Protein, PDBID: 6M1D; C: Nintedanib, D: Darunavir on Mpro, PDBID: 5R82; E: Nintedanib; F: Quercetin on Spike Protein. PDBID: 1ZV8

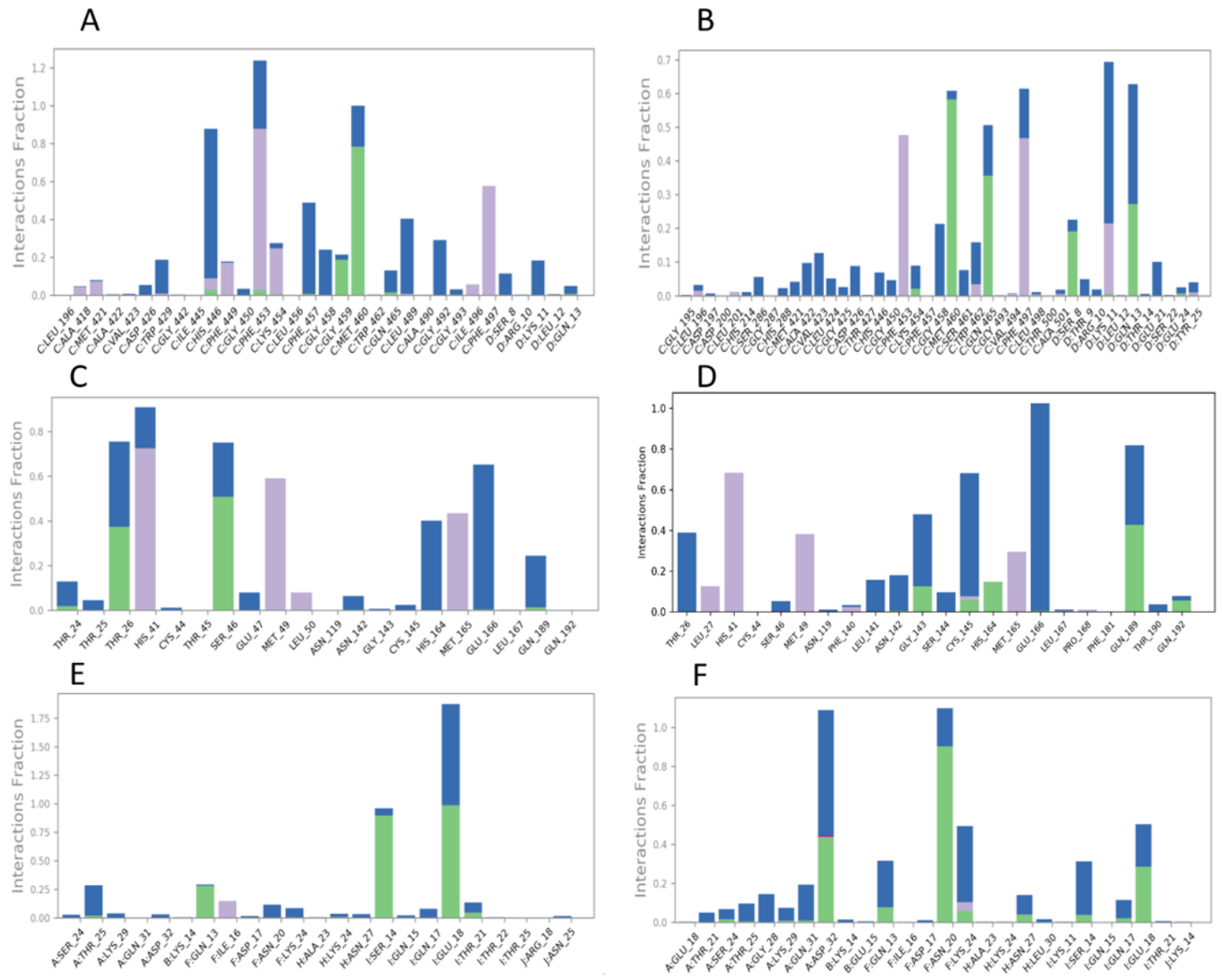

Figure 3

Protein-ligand contacts A: Nintedanib, B: Baricitinib on ACE2 Protein, PDBID: 6M1D; C: Nintedanib, D: Darunavir on Mpro, PDBID: 5R82; E: Nintedanib; F: Quercetin on Spike Protein. PDBID: 1ZV8

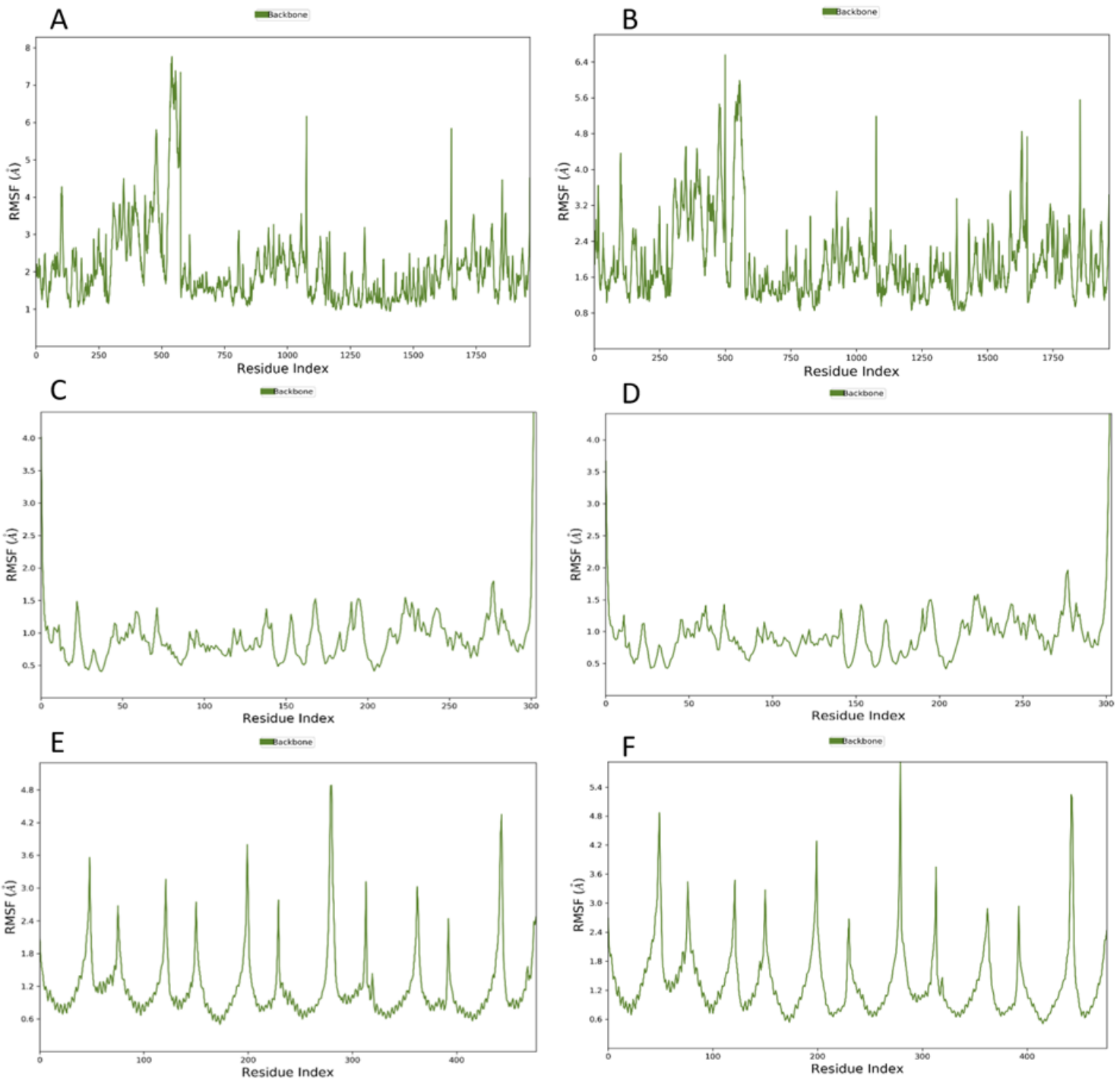

Figure 4

Protein RMSF A: Nintedanib, B: Baricitinib on ACE2 Protein, PDBID: 6M1D; C: Nintedanib, D: Darunavir on Mpro, PDBID: 5R82; E: Nintedanib; F: Quercetin on Spike Protein. PDBID: 1ZV8

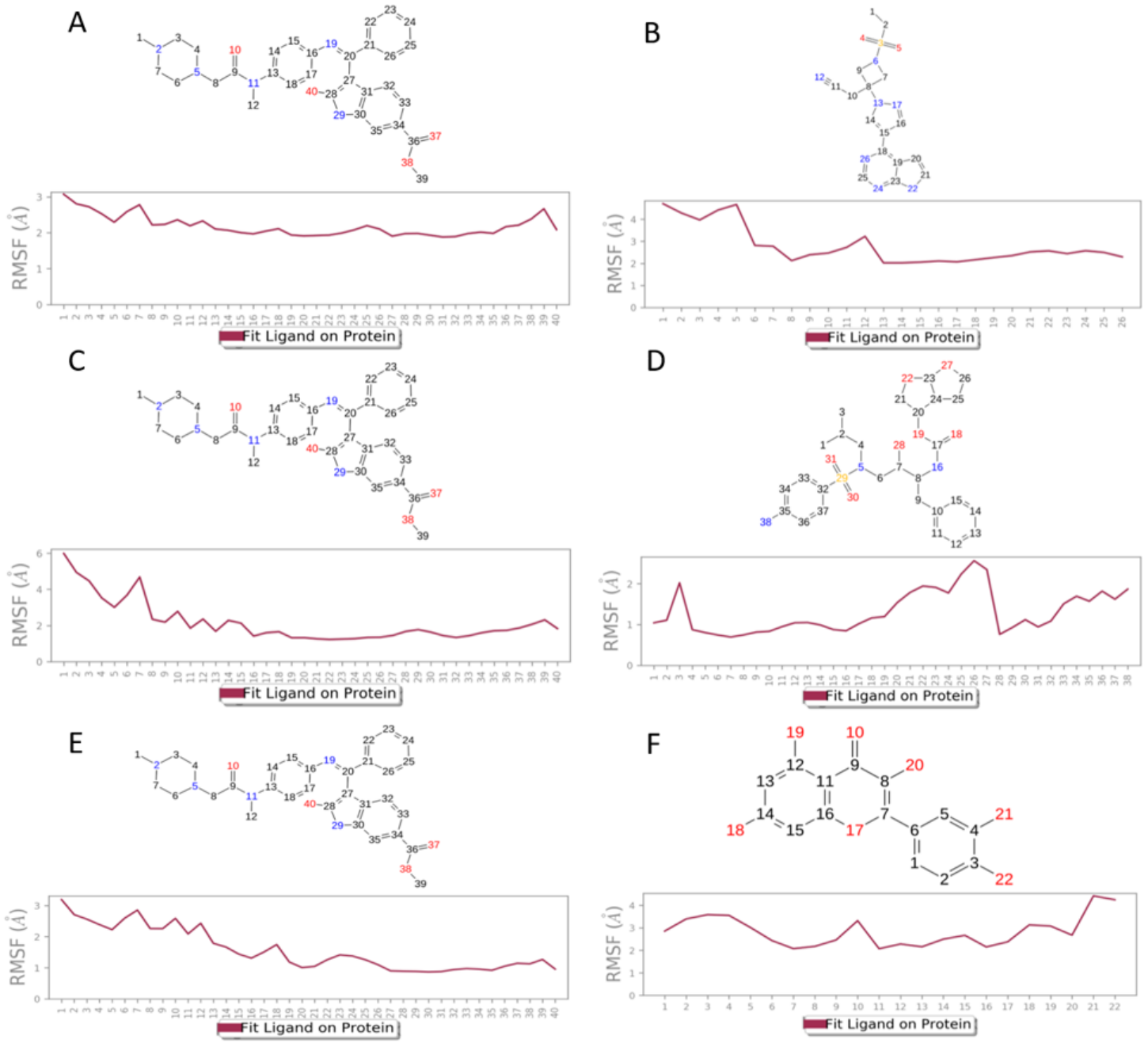

Figure 5

Ligand RMSF A: Nintedanib, B: Baricitinib on ACE2 Protein, PDBID: 6M1D; C: Nintedanib, D: Darunavir on Mpro, PDBID: 5R82; E: Nintedanib; F: Quercetin on Spike Protein. PDBID: 1ZV8

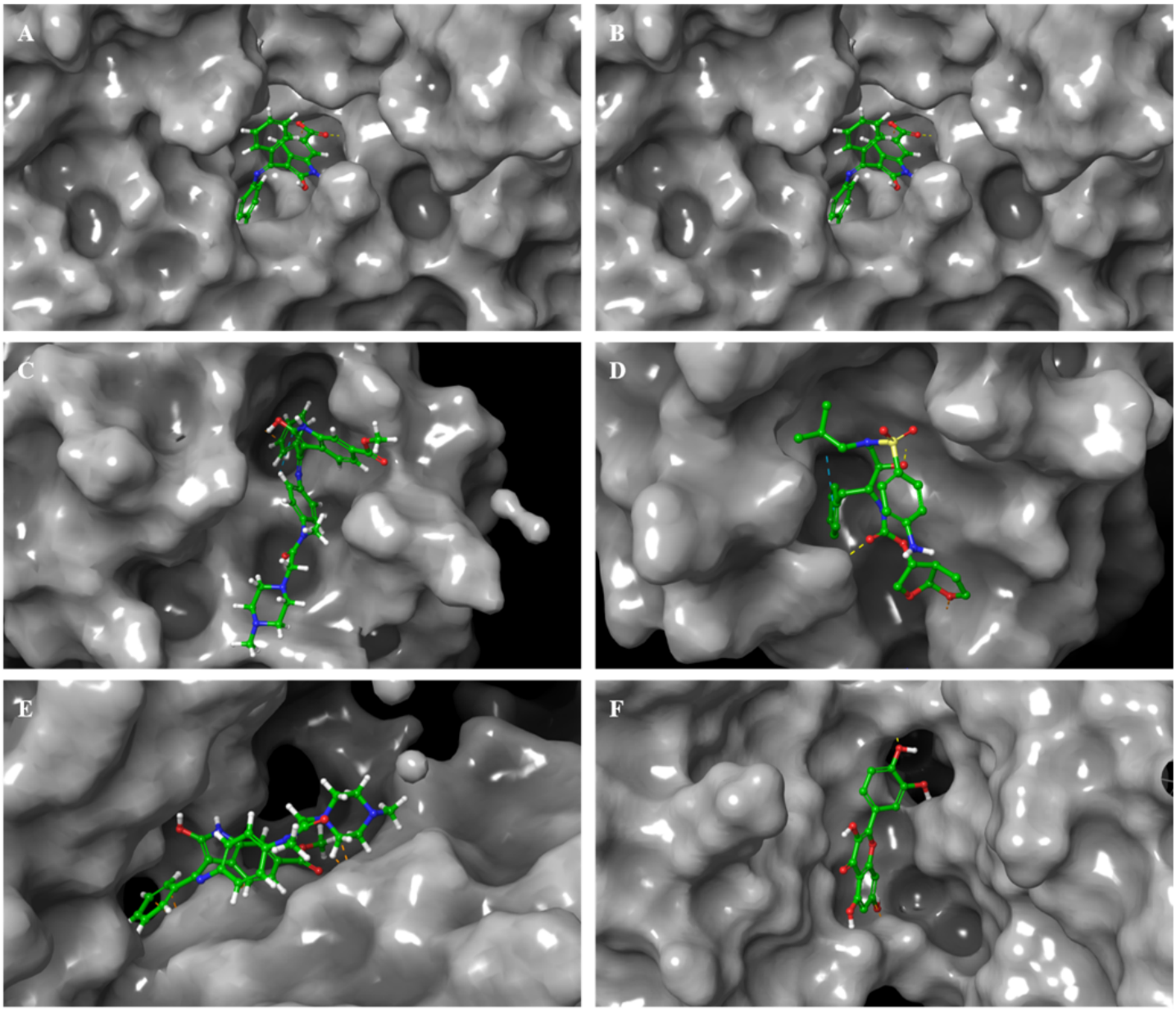

Figure 6

Ligand 3D interactions A: Nintedanib, B: Baricitinib on ACE2 Protein, PDBID: 6M1D; C: Nintedanib, D: Darunavir on Mpro, PDBID: 5R82; E: Nintedanib; F: Quercetin on Spike Protein. PDBID: 1ZV8

Supplementary Files

This is a list of supplementary files associated with this preprint. Click to download.

- GAbstract.tif